Mode-resolved gain analysis and lasing in multi-supermode multi-core fiber laser

Clémence Jollivet,[1,*] Arash Mafi,[2] Daniel Flamm,[3] Michael Duparré,[3] Kay Schuster,[4] Stephan Grimm,[4] and Axel Schülzgen[1]

[1]*CREOL, the College of Optics and Photonics, University of Central Florida, Orlando, FL, USA*
[2]*Department of Physics and Astronomy and Center for High Technology Materials, University of New Mexico, Albuquerque, NM, USA*
[3]*Institute of Applied Optics, Friedrich Schiller University, Fröbelstieg 1, Jena, Germany*
[4]*Leibniz Institute of Photonic Technology e.V., A.-Einstein-Str. 9, Jena, Germany*
**jollivet@creol.ucf.edu*

Abstract: Multi-core fibers (MCFs) with coupled-cores are attractive large-mode area (LMA) specialty fiber designs that support the propagation of a few transverse modes often called supermodes (SMs). Compared to other LMA fibers, the uniqueness of MCF arises from the higher degrees of design space offered by a multitude of core-array geometries, resulting in extended flexibility to tailor SM properties. To date, the use of MCF as gain media has focused on lasers that operate in only one selected SM, typically the lowest order in-phase SM, which considerably limited the potential of these multi-core structures. Here, we expand the potential of MCF lasers by investigating multi-SM amplification and lasing schemes. Amplifier and laser systems using a 7 coupled-cores Yb-doped MCF as gain medium were successfully designed and assembled. Individual SM could be decomposed using the correlation filter technique mode analysis and the modal amplification factors (γ_i) were recorded. With access to amplification characteristics of individual transverse modes, a monolithic MCF laser was demonstrated that operates simultaneously on the two SMs carrying the highest optical gain.

OCIS codes: (060.3510) Lasers, fiber; (060.4005) Microstructured fibers; (060.2270) Fiber characterization.

References and links

1. A. F. Gmitro and D. Aziz, "Confocal microscopy through a fiber-optic imaging bundle," Opt. Lett. **18**(8), 565–567 (1993).
2. D. J. Rchardson, J. M. Fini, and L. E. Nelson, "Space division multiplexing in optical fibres," Nat. Photonics **7**(5), 354–362 (2013).
3. D. Richardson, J. Nilsson, and W. A. Clarkson, "High power fiber lasers: current status and future perspectives," J. Opt. Soc. Am. B **27**(11), B63–B92 (2010).
4. J. E. Antonio-Lopez, Z. S. Eznaveh, P. LiKamWa, A. Schülzgen, and R. Amezcua-Correa, "Multicore fiber sensor for high-temperature applications up to 1000°C," Opt. Lett. **39**(15), 4309–4312 (2014).
5. C. Xia, R. Amezcua Correa, N. Bai, E. Antonio-Lopez, D. May Arrioja, A. Schülzgen, M. Richardson, J. Linares, C. Montero, E. Mateo, X. Zhou, and G. Li, "Hole-assisted few-mode multicore fiber for high-density space-division multiplexing," IEEE Photon. Technol. Lett. **24**(21), 1914–1917 (2012).
6. S. Zheng, G. Ren, Z. Lin, and S. Jian, "Mode-coupling analysis and trench design for large-mode-area low-cross-talk multicore fiber," Appl. Opt. **52**(19), 4541–4548 (2013).
7. K. S. Abedin, T. F. Taunay, M. Fishteyn, D. J. DiGiovanni, V. R. Supradeepa, J. M. Fini, M. F. Yan, B. Zhu, E. M. Monberg, and F. V. Dimarcello, "Cladding-pumped erbium-doped multicore fiber amplifier," Opt. Express **20**(18), 20191–20200 (2012).
8. F. Y. M. Chan, A. P. T. Lau, and H. Y. Tam, "Mode coupling dynamics and communication strategies for multi-core fiber systems," Opt. Express **20**(4), 4548–4563 (2012).
9. C. Guan, L. Yuan, and J. Shi, "Supermode analysis of multicore photonic crystal fibers," Opt. Commun. **283**(13), 2686–2689 (2010).
10. C. Xia, N. Bai, I. Ozdur, X. Zhou, and G. Li, "Supermodes for optical transmission," Opt. Express **19**(17), 16653–16664 (2011).

#210303 - $15.00 USD Received 25 Sep 2014; revised 16 Nov 2014; accepted 21 Nov 2014; published 26 Nov 2014

11. P. K. Cheo, A. Liu, and G. G. King, "Ä high-brightness laser beam from a phase-locked multicore Yb-doped fiber laser array," IEEE Photon. Technol. Lett. **13**(5), 439–441 (2001).
12. L. Li, A. Schülzgen, S. Chen, V. L. Temyanko, J. V. Moloney, and N. Peyghambarian, "Phase locking and in-phase supermode selection in monolithic multicore fiber lasers," Opt. Lett. **31**(17), 2577–2579 (2006).
13. L. Li, A. Schülzgen, H. Li, V. L. Temyanko, J. V. Moloney, and N. Peyghambarian, "Phase-Locked Multicore All-Fiber Lasers: Modeling and Experimental Investigation," J. Opt. Soc. Am. B **24**(8), 1721 (2007).
14. X. Zhu, A. Schülzgen, L. Li, H. Li, V. L. Temyanko, J. V. Moloney, and N. Peyghambarian, "Birefringent in-phase supermode operation of a multicore microstructured fiber laser," Opt. Express **15**(16), 10340–10345 (2007).
15. K. Hamamoto, E. Gini, C. Holtmann, and H. Melchior, "Single-transverse-mode active multi- mode interferometer 1.45 μm high power laser diode," Appl. Phys. B **73**(5-6), 571–574 (2001).
16. H. J. Baker, J. R. Lee, and D. R. Hall, "Self-imaging and high-beam-quality operation in multi-mode planar waveguide optical amplifiers," Opt. Express **10**(6), 297–302 (2002).
17. W. S. Pelouch, D. D. Smith, J. E. Koroshetz, I. T. Mckinnie, J. R. Unternahrer, S. W. Henderson, and W. R. Scharpf, "Self-imaging in waveguide lasers and amplifiers", OSA Topical Meeting on Advanced Solid State Lasers, 6–9 (Optical Society of America, Washington, D. C., 2002).
18. X. Zhu, A. Schülzgen, H. Li, L. Li, Q. Wang, S. Suzuki, V. L. Temyanko, J. V. Moloney, and N. Peyghambarian, "Single-Transverse-Mode Output from a Fiber Laser Based on Multimode Interference," Opt. Lett. **33**(9), 908–910 (2008).
19. Y. Huo and P. K. Cheo, "Analysis of transverse mode competition and selection in multicore fiber lasers," J. Opt. Soc. Am. B **22**(11), 2345–2349 (2005).
20. A. S. Kurkov, S. A. Babin, I. A. Lobach, and S. I. Kablukov, "Mechanism of mode coupling in multicore fiber lasers," Opt. Lett. **33**(1), 61–63 (2008).
21. K. Schuster, S. Unger, C. Aichele, F. Lindner, S. Grimm, D. Litzkendorf, J. Kobelke, J. Bierlich, K. Wondraczek, and H. Bartelt, "Material and technology trends in fiber optics," Adv. Opt. Technol. **3**, 447–468 (2014).
22. A. Benoit, R. Dauliat, K. Schuster, S. Grimm, R. Jamier, F. Salin, and P. Roy, "Optical fiber microstructuration for strengthening single-mode laser operation in high power regime," Opt. Eng. **53**(7), 071817 (2014).
23. A. W. Snyder, "Coupled-mode theory for optical fibers," J. Opt. Soc. Am. **62**(11), 1267–1277 (1972).
24. T. Kaiser, D. Flamm, S. Schröter, and M. Duparré, "Complete modal decomposition for optical fibers using CGH-based correlation filters," Opt. Express **17**(11), 9347–9356 (2009).
25. W. H. Lee, "Sampled fourier transform hologram generated by computer," Appl. Opt. **9**(3), 639–643 (1970).

1. Introduction

During the past decade, a wide variety of micro-structured multi-core waveguide designs have been demonstrated, enabling to tailor light propagation properties in order to benefit an ever-increasing number of applications in the field of high-resolution imaging [1], fiber optic communications [2], fiber lasers and amplifiers [3] and fiber-based sensors [4].

Two categories of multi-core fibers (MCF) can be distinguished. On one hand, isolated-cores MCF designs combine several single-emitter cores to ensure low-cross talk and high modal density for example through hole-assisted and trench-assisted designs [5,6]. Applications include highly efficient data transmission and in-fiber multi-channel amplification [7]. On the other hand, MCF designed with small core-to-core (pitch) values can exhibit strong coupling between individual cores. During light propagation, evanescent field coupling occurs resulting in the formation of so-called supermodes (SMs). SMs are defined as linear combinations of the LP modes guided in each individual core and constitute an orthonormal basis [8,9].

In the present study, we focus on coupled-core MCFs. In the case where individual cores satisfy the single-mode condition, these MCFs form few-modes systems in which the number of guided SMs equals the number of cores (times two if polarization is considered). SMs offer both large mode-effective-area and high mode density placing MCFs within the category of large-mode area (LMA) fiber designs. Among few-modes LMA fibers, MCFs are unique for the significantly higher number of degrees of freedom available when designing the core array structure i.e. number, size, pitch and arrangements of individual cores, offering unmatched control over light propagation properties. Besides being a good candidate for communication applications [3,10], coupled-cores MCFs have been successfully used in fiber laser systems delivering high brightness laser beams after selection of the in-phase SM [11–14].

While MCF amplifiers or lasers with integrated single supermode selection [11–14] can be viewed as the digital analog of large mode are fiber amplifiers and lasers with fundamental mode selection, the investigated scheme of simultaneous multi-supermode amplification and

#210303 - $15.00 USD Received 25 Sep 2014; revised 16 Nov 2014; accepted 21 Nov 2014; published 26 Nov 2014

lasing is the equivalent of a planar waveguide [15–17] or fiber laser [18] with multimode gain section and single transverse mode emission. While fiber lasers with multimode gain section [18] can provide perfect beam quality (M^2 = 1.01), high efficiency, and a low emission bandwidth, their performance is strongly affected by external perturbations. Multicore gain sections are studied here since they promise advantages over conventional multimode gain section such as improved mode control and reduced vulnerability to external perturbations due to improved stability of multi-(super)mode interference effects.

To date, the complexity of simultaneous multi-mode lasing has been the main limitation to further explore the full potential of MCF-based lasers in practice. While several numerical studies were reported revealing SM competition mechanisms in MCF-based lasers [19,20], the lack of experimental techniques allowing to access individual SM amplification characteristics persists.

Here, individual SM amplification factor, competition mechanisms and multi-SM simultaneous lasing in MCFs were experimentally investigated in a 7 coupled-cores Yb-doped MCF.

2. Supermodes in coupled-cores fiber

An all-solid 7-cores design embedded in a hexagonal-shaped cladding was selected. The long diagonal was measured to be 125 µm in diameter, ensuring a good compatibility with conventional fibers. In Fig. 1(a), an image of the fiber facet was recorded under a microscope. The core diameter (d) and fiber pitch (Λ) were measured to be 5.9 µm and 9.3 µm (± 0.1 µm) respectively. The cores of the MCF were doped with Yb^{3+} atoms (~$4.5.10^{25}$ /m^3) and fabricated employing the REPUSIL technique [21,22]. To evaluate the uniformity of the doping across the 7 cores, the refractive index of the MCF was measured using a profilometer (by InterFiber Analysis). Results shown in Fig. 1(b) and (c) were measured at 1 µm light wavelength and confirm the good uniform of the doping profile across all the 7-cores within a range of Δn = ± $2.5.10^{-4}$. At this wavelength, the MCF numerical aperture was found to be ~0.1, yielding to a V-parameter of ~1.8 and individual cores operating in the single-mode regime. According to the small MCF pitch, evanescent core coupling occurs resulting in the formation of SMs.

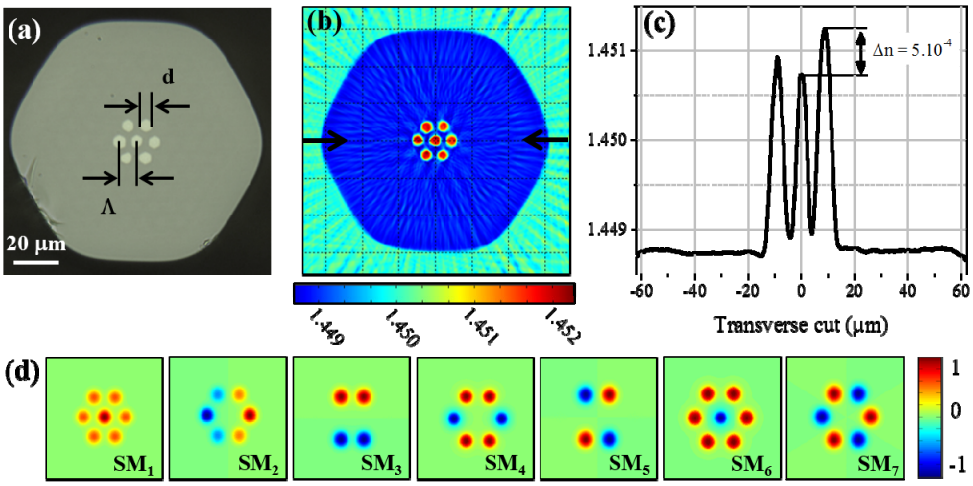

Fig. 1. (a) Microscope image of the MCF facet. (b) Measured refractive index profile at 1 µm light wavelength. (c) Transverse cut extracted from the 2D refractive index profile (at the location indicated with black arrows). (d) Calculated electric field of the 7 SMs supported by the MCF using the measured index profile.

Using a finite-element mode solver (Fimmwave by PhotonDesign), the SMs were calculated using the measured fiber dimensions and indices at 1 µm. Results are presented in

#210303 - $15.00 USD Received 25 Sep 2014; revised 16 Nov 2014; accepted 21 Nov 2014; published 26 Nov 2014

Fig. 1(d) showing the calculated fields of the 7 SMs (note that each SM is two-fold polarization degenerated). Similar to conventional step-index fibers, this MCF is a few-modes fiber, in which the combination of excited SM is influenced by the core alignment, the input mode overlap and external perturbations such as coiling. Outperforming step-index few-mode fibers, the excited SM content in MCF can be chosen by tailoring the MCF design combined with excitation control without employing additional mode conversion or mode selection techniques. In theory, the 7-cores MCF shown in Fig. 1 can act as a two modes fiber if one would excite the center core only. In such case, only the SMs with non-zero center intensity in the center core, fulfilling the mode overlap conditions, can be excited which, according to Fig. 1(d), correspond to SM_1 and SM_6.

In practice, a conventional single-core, step-index, single-mode fiber (SMF, SM980 by Thorlabs), matched to the center of the MCF, was fusion spliced to both ends of a 90 cm long MCF segment, forming a monolithic chain SMF-MCF-SMF. Using a broadband light source emitting around the wavelength of 1 μm, light transmission was measured with an optical spectrum analyzer. Results, presented in Fig. 2(a), show the characteristic multi-mode interference occurring in few-mode fibers and the observed periodic modulation confirms that only a few SMs are excited and propagate in the MCF. Accounting for background losses (~2 dB), mainly attributed to splices with the SMF and absorption losses also ~2 dB up to ~1060 nm, overall fiber losses along this fiber segment can be evaluated around 1 dB. However, it is important to note that individual mode losses cannot be directly accessible in practice.

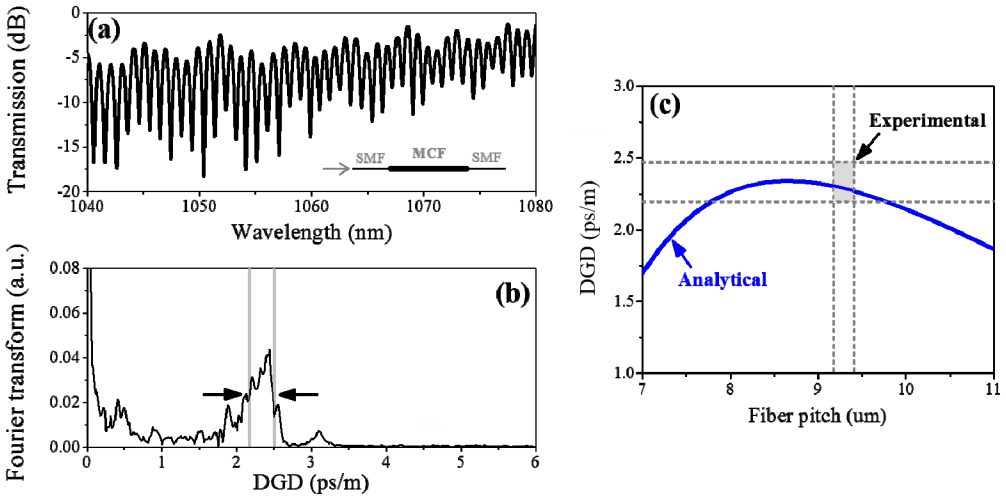

Fig. 2. (a) Light transmission measured through a chain SMF-MCF-SMF showing the characteristic multi-mode interference pattern of the MCF. (b) Fourier transform of (a) showing a maximum, signature of two interfering SMs at a DGD comprised between 2.2 and 2.5 ps/m. (c) Comparison between analytically calculated (blue line) and experimentally measured (grey area) DGD between SM1 and SM6 as function of the MCF pitch.

To identify the SMs excited ad guided in the MCF, analytical and experimental values of the differential group delay (DGD) between propagating modes were obtained and compared. Experimentally, the DGD was obtained after calculating the Fourier transform of the multi-mode interference transmission (Fig. 2(a)). The results in Fig. 2(b) show one maximum indicating two interfering SMs with a DGD comprised between 2.2 and 2.5 ps/m. In addition, a semi-analytical model based on the coupled mode theory [23] was developed in order to predict the properties of light propagation in the SMF-MCF-SMF chain. Using the equations detailed in Appendix, the transmission can be calculated from

$$T(\nu) = 1 - 4P_1P_6 \sin^2\left(2\sqrt{7}\tilde{c}(\nu)L\right), \quad (1)$$

#210303 - $15.00 USD Received 25 Sep 2014; revised 16 Nov 2014; accepted 21 Nov 2014; published 26 Nov 2014

where P_1 (also labeled ρ^2_1) and P_6 (ρ^2_6) correspond to the fraction of light carried by SM_1 and SM_6 respectively, L is the MCF segment length, $\tilde{c}$ is the core-coupling coefficient and ν is the light frequency. Using the present pair SMF-MCF, calculated values were $P_1 = 0.31$ and $P_6 = 0.69$. The DGD between SM_1 and SM_6 (labeled c_1 in the analytical development in Appendix) was calculated from the derivative of $\tilde{c}$ with respect to the light frequency. The experimental and analytical values of the DGD are represented in Fig. 2(c) using the shaded area and the blue line respectively, as function of the MCF pitch. Measured and calculated values show a good agreement confirming that mainly SM_1 and SM_6 are excited and propagate in the MCF.

Next, the correlation filter technique (CFT), widely employed to perform mode analysis in optical fibers [24], was used in order to evaluate the relative amount of light carried by individual SMs, labeled ρ^2_i, whith i the respective SM index. A schematic of the CFT is presented in Fig. 3(a).

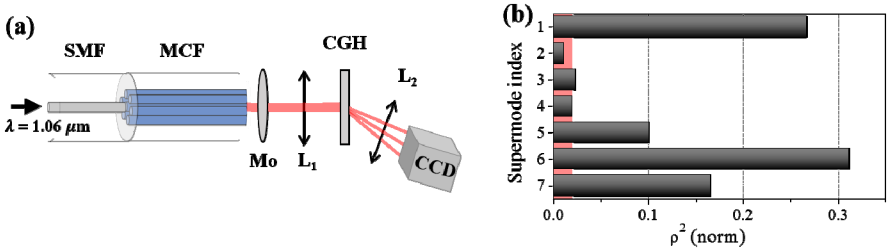

Fig. 3. (a) Schematic of the supermode analysis experiment with: a laser source emitting around 1.06 µm wavelength, coupled in a single-mode fiber (SMF) with Mo: Microscope objective, L_1: imaging lens, CGH: computer generated hologram, L_2: Fourier lens. (b) Results of the MCF mode analysis showing the normalized power distribution among the excited supermodes. The red area indicates the lowest detection limit of ± 2% when measuring ρ^2 values.

A narrow-line width laser emitting at 1.06 µm was coupled in the SMF fusion spliced to the MCF segment. The beam emerging from the MCF was magnified and imaged on a specifically designed computer generated hologram (CGH) [25]. The diffracted light, containing information regarding modal powers (ρ^2_i), was imaged using a Fourier lens (L_2) on a CCD and analyzed. The SM decomposition results are presented in the bar diagram in Fig. 3(b) yielding $\rho_1^2 = 27\%$ and $\rho_6^2 = 32\%$. During the mode decomposition, the lowest detection limit of ± 2%, mainly limited by the CCD sensitivity at this wavelength, was illustrated with the red area in Fig. 3(b). According to the mode analysis results, up to 16% and 10% of the total power was also found to be carried by SM_7 and SM_5. This can be explained by imperfections during the experimental realization such as small input mode-field mismatch between the commercial SMF employed (5.8 µm core diameter and ~0.13 numerical aperture) and the MCF, by a slight offset during the splicing process, or by inter-SM coupling during propagation, for instance induced by micro-bending. The power population in SM_5 and SM_7 could have also been anticipated from the spurious peaks in the Fourier response (Fig. 2(b)) around 0.5 ps/m and 3.1 ps/m.

3. Analysis of individual supermode amplification factors

Since all supermodes that propagate in the optically excited MCF utilize the same inversion, the amplification coefficients are not independent of each other. Here, we attempt to measure effective modal amplification coefficients γ_i and their dependence on external perturbations. Here, we propose an approach to evaluate the values of γ_i in a multi-mode amplifier. The schematic of the experiment is represented in Fig. 4. A (2 + 1)x1 pump combiner was used to couple both signal (seed laser at 1.06 µm) and pump (multimode laser diode at 976 nm) in the MCF. The fiber-coupled pump light was delivered via a fiber with 105 µm core diameter. After the combiner, the pump light was maintained in the first cladding of a double-clad (DC) fiber with a diameter of 105 µm. The size of the core of the DC fiber was matching the SMF

#210303 - $15.00 USD Received 25 Sep 2014; revised 16 Nov 2014; accepted 21 Nov 2014; published 26 Nov 2014

employed in Section 2. The signal port of the combiner was fusion spliced to a 90 cm long MCF segment which has been uncoated to allow efficient cladding pump absorption. The laser seed from the SMF was coupled to the center core of the MCF.

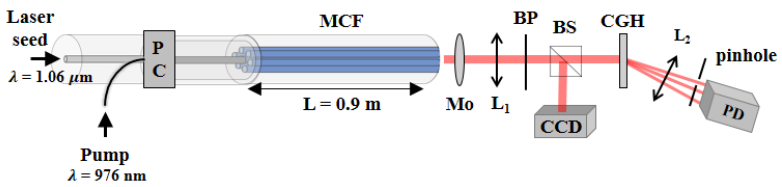

Fig. 4. Schematic of the experiment to measure γ_i. The all-fiber pump combiner (PC) was used to simultaneously couple the seed and the pump light in the MCF. Mo: microscope objective; L_2: magnification lens (m = 75); BP: band-pass filter isolating the signal from the residual pump; BS: beam splitter; CGH: computer generated hologram; L_2: Imaging lens; 200 μm diameter pinhole; PD: photodetector.

To measure the modal amplification factor, the CFT analysis previously described in Section 2 (Fig. 3(a)) was used with the addition of a bandpass filter to cut-off the residual pump, a beam splitter to direct a fraction of the beam on a CCD for real-time monitoring of the MCF near-field image and a pair of pinhole and photodetector. The 200 μm diameter pinhole was inserted after L_2 to isolate the correlation answer from one SM. To do so, a CCD was used instead of the photodetector during the alignment procedure, ensuring the selection of a single correlation answer. The photodetector was used to record the fraction of seed power carried by the selected SM while changing the pump power (the seed power remained unchanged). Measurement results of γ_i, the amplification factor of the i^{th} mode, are presented in Fig. 5(a) for SM_1 and SM_6. During seed amplification, these two supermodes exhibited different modal amplification factor values such that $\gamma_1 > \gamma_6$. For 3.3 W of launched pump power, it was measured that γ_1~12 dB which was more than 2 dB higher than γ_6.

This trend was verified by performing the complete CFT analysis, after exchanging the pair pinhole-photodetector by the CCD, during amplification at 3.3 W pump power. The mode analysis results, summarized in Fig. 5(b), were compared between the pump OFF measurement (Fig. 3(b)) with the pump ON at 3.3 W (black arrow in Fig. 5(a)) represented with shaded and plain bars respectively. While the non-amplified seed was composed of a dominant SM_6, during amplification using 3.3 W of pump power, SM_1 became dominant carrying almost 40% of the amplified seed compared to ρ_6^2 ~25%. This measurement confirmed the mode amplification factor trend found to be $\gamma_1 > \gamma_6$. The total beam profile emerging the MCF are displayed in Fig. 5(b) (right) without (top) and with amplification (bottom). The good radial uniformity of the amplified beam is consistent with a dominant SM_1.

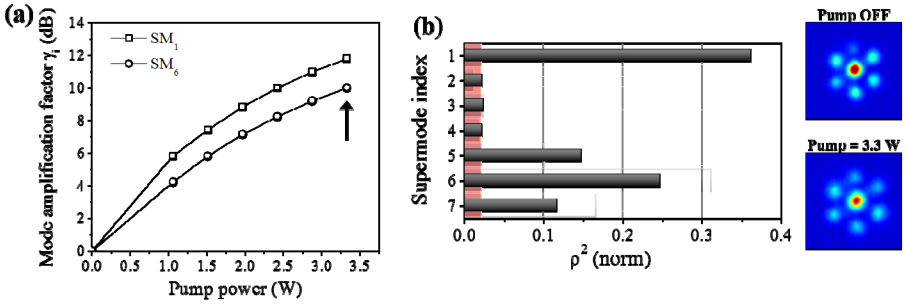

Fig. 5. (a) Measured mode amplification factor γ carried by in SM_1 (square markers) and SM_6 (circle markers) measured individually for various pumping levels. (b) Mode analysis of the delivered seed during pump at P = 3.3 W. Results illustrated by the dark grey bars are compared to the mode content at P = 0 W (shaded light grey bars). The seed profile emerging the MCF was measured on the CCD (right) without and with pump amplification.

#210303 - $15.00 USD Received 25 Sep 2014; revised 16 Nov 2014; accepted 21 Nov 2014; published 26 Nov 2014

To expand this study further, modal amplification factor were measured for different MCF mode mixings induced with external perturbations while preserving the same amplifier design. The goal was to monitor the evolution of the modal amplification factors as the seed power became gradually distributed among the supermodes. To do so, the mode content in the MCF has been externally perturbed using small amounts of coil (Fig. 6(a)) and stress (Fig. 6(b) using a microscope slide). In each case, the beam emerging from the MCF was recorded with the CCD and the corresponding mode content was measured with the CFT analysis. Results obtained in the case where only the seed light was propagating in the MCF (no pumping) are illustrated in Fig. 6(a) and 6(b) respectively. According to the distortions in the measured beam profiles and from the mode decomposition results, it clearly appears that additional SM mixing was induced by external perturbations. Using the experiment detailed in Fig. 4, γ_i values were measured and results are shown in Fig. 6(c) and (d) respectively. Similarly to the results obtained with the straight and unperturbed MCF (Fig. 5(a)), different SM are characterized by different γ_i values. However, on common trend can be highlighted from these measurements. Regardless of the passive mode content. i.e. even when SM_1 is not guided dominantly, for instance in Fig. 6(a) and 6(c), SM_1 was measured with the highest mode amplification factor,. Also, while the absolute modal amplification factor differs between the straight (γ_1 = 11.8 dB), coiled (γ_1 = 7.6 dB) and stressed (γ_1 = 8.8 dB) MCF, the relative order remains unchanged during pumping with $\gamma_1 > \gamma_6 > \gamma_7 > \gamma_5$.

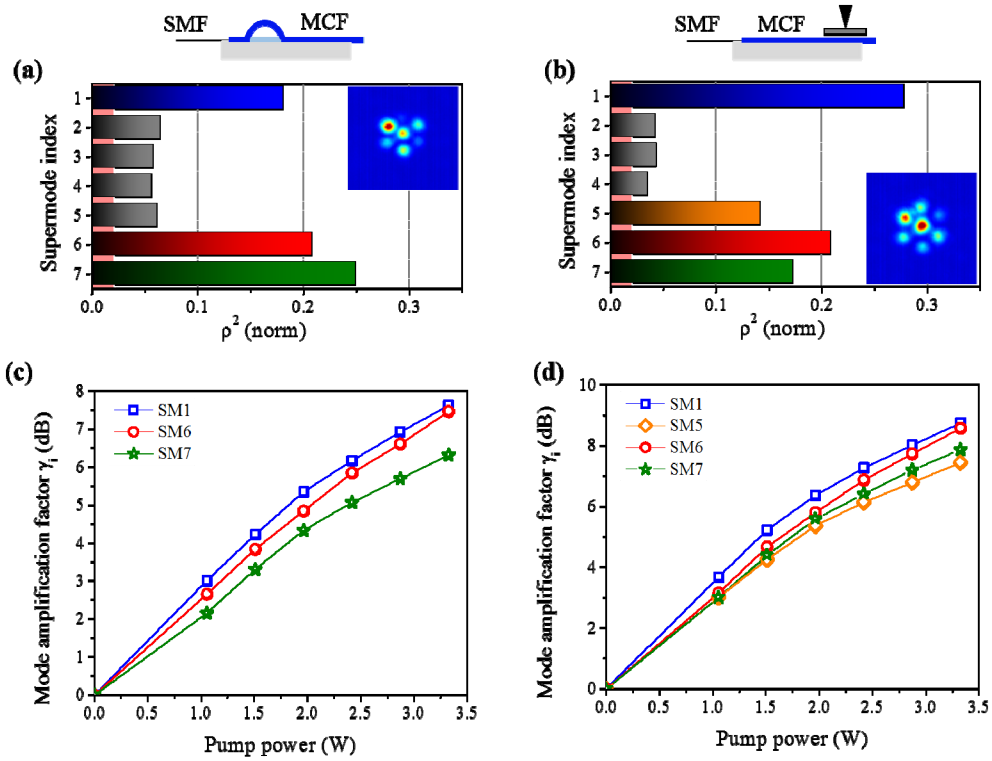

Fig. 6. Results of CFT mode analysis of the seed laser (1.06 µm) under (a) coil and (b) stress (pump is OFF). The corresponding MCF near field recorded on the CCD is illustrated. Results of the mode amplification factor measurement for various pump levels in the coiled (c) and stressed (d) MCF. γ_i values were recorded for SM_1 (blue squares), SM_6 (red circles), SM_7 (green stars) and SM_5 (orange diamonds).

Thus, while the "passive" SM content (measured with the seed light only) depended on the in-coupling alignment, the mode overlap and was influenced by external perturbations leading to SM coupling, it was demonstrated that, regardless of the configuration, the amplification

#210303 - $15.00 USD Received 25 Sep 2014; revised 16 Nov 2014; accepted 21 Nov 2014; published 26 Nov 2014

factor of SM_1 was always the highest, followed by SM_6 and SM_7 and SM_5. While individual supermodes have different effective amplification coefficients, that are influenced by their respective overlap with the doping profile, all supermodes have been found to experience strong gain and can, therefore, simultaneously contribute to the MCF laser emission. This can result in a more effective utilization of the total pump induced inversion compared to conventional MCF lasers that are tailored to single supermode operation with limited overlap between the lasing supermode and the outer cores.

4. Multi-supermode lasing in MCF

To date, simultaneous lasing of multiple SM in MCF have not been exploited due to the lack of experimental means to characterize and understand unstable and complex laser behavior. In this section, the influence of core-selective feedback elements on different multi-SM lasing regimes was determined. To do so, the 90 cm long MCF segment used in Section 3 was spliced between two fiber Bragg gratings (FBG) written in the SMF, creating a fiber laser cavity as illustrated in Fig. 7(a). The FBG pair consisted of a high reflector (HR), 99% reflective at the Bragg wavelength λ = 1029.65 nm ($\Delta\lambda$ = 0.16 nm) and a low reflector (LR) providing 21% of feedback at a wavelength of 1029.95 nm ($\Delta\lambda$ = 0.05 nm). A cladding pumping scheme was selected to maintain a uniform illumination for each core and efficient pump absorption was achieved with the hexagonal shaped cladding.

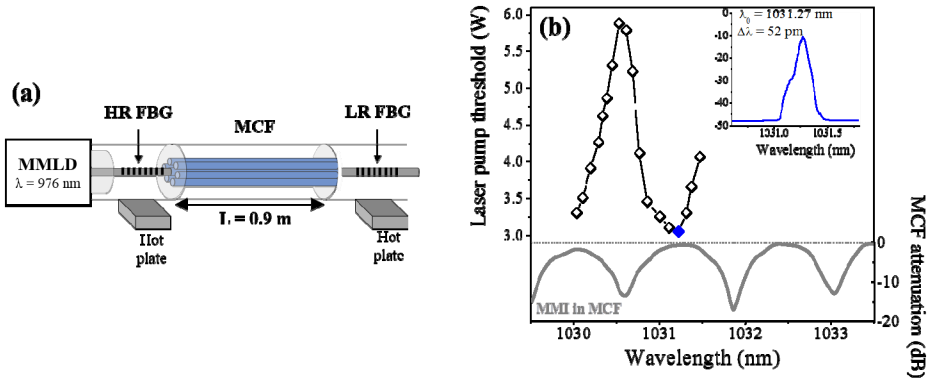

Fig. 7. (a) Schematic of the monolithic multicore fiber laser with MMLD: multimode laser diode. (b) Measured laser threshold vs emission wavelength (black diamonds) compared with the SMI pattern measured in Fig. 2(a) (plain grey line). The laser emission spectrum measured at λ = 1031.22 nm (filled blue diamond marker) is shown in inset.

According to the findings in Section 3, SM_1 and SM_6 are expected to carry the highest amplification factors. Moreover, from the multi-mode interference (MMI) measurement (Fig. 2(a)), light transmission through a chain SMF-MCF-SMF was characterized by a high-contrast spectral modulation. While pumping the MCF laser, both FBGs were fixed on hot plates providing the ability to tune the laser wavelength across a total bandwidth of 1.4 nm, which is larger than one MMI period. For each laser emission wavelength, the pump threshold was measured and results are shown in Fig. 7(b) using diamond-shaped markers. For comparison, the measured MMI transmission through the SMF-MCF-SMF chain is shown on the same graph (grey line, right scale). While the laser wavelength was tuned, the cavity feedback changed according to the MMI pattern. The lowest laser threshold measured for λ_L = 1031.27 nm, corresponds to a MMI maximum, while the threshold at the neighboring transmission minimum is found to be twice as high. The laser spectrum corresponding to the lowest threshold operation is shown in the inset of Fig. 7(b) indicating a 52 pm laser linewidth that is dictated by the LR FBG.

As a result, it was demonstrated that there is direct correlation between MMI in few-modes fiber systems and the laser operation when multiple SM oscillate simultaneously.

#210303 - $15.00 USD Received 25 Sep 2014; revised 16 Nov 2014; accepted 21 Nov 2014; published 26 Nov 2014

5. Summary and conclusion

To summarize, mode-resolved amplification factor and multi-SM lasing in Yb-doped MCF supporting 7 SMs at λ = 1.06 μm were investigated. The proposed approach to resolve mode amplification factors using CFT and a pair pinhole-photodetector can easily be generalized to further investigate mechanisms of gain dynamics and competition in any few-modes fiber amplifier and laser system. Using a novel coupled-core multi-core fiber amplifier, we demonstrated the ability to measure the amplification factors (γ_i) of each of the transverse mode simultaneously amplified. The measured γ_i values could be used to gain insight in the evolution of the individual amplified mode content while the supermode amplifier was being perturbed. In particular, knowledge of the γ_i coefficient can directly contribute to a better understanding of multi-SM monolithic MCF lasers. A MCF laser cavity was successfully assembled and fine tuning of the lasing mode content was demonstrated. Control and enhancement of the laser performances were proven and discussed.

Appendix

The beam propagation equation of the 7-coupled-cores fiber can be written as

$$\frac{dE_i}{dz} = -i\left(\sum_{j=1}^{7} M_{ij}E_j\right) \tag{2}$$

where i = 1 is the center core and i = 2,…,7 represents the surrounding cores, E_i is the field of the supermodes (eigenvectors), $M_{ii} = \tilde{\beta}_i$ for i = 1,…,7 the effective propagation constants (eigenvalues) and $M_{i1} = M_{1i} = M_{i,i-1} = M_{i-1,i} = \tilde{c}$ for i = 2,…,7 the core-coupling coefficients.

Considering a single-core, single-mode fiber matched to the center core of the MCF, only SM with non-zero intensity in the center core will be excited. The corresponding eigenvectors V can be expressed as

$$V_1 = \left(-1+\sqrt{7},1,1,1,1,1,1\right) \text{and } V_6 = \left(1+\sqrt{7},-1,-1,-1,-1,-1,-1\right). \tag{3}$$

The SM fields, respectively labeled E_1 and E_6, can be defined as $E_i(L) = E_i(0)e^{i\tilde{\beta}_i L}$ with L the MCF propagation length and $\tilde{\beta}$, the effective propagation constant, defined by

$$\tilde{\beta}_1 = \beta + (1-\sqrt{7})\tilde{c} \text{ and } \tilde{\beta}_6 = \beta + (1+\sqrt{7})\tilde{c}. \tag{4}$$

Light transmission in the MCF, collected using the same SMF, can be calculated using

$$T = \left|E_1^*(0)E_1(\mathrm{L}) + E_6^*(0)E_6(\mathrm{L})\right|^2. \tag{5}$$

Expressed in terms of light frequency, it can be written as

$$T(\nu) = 1 - 4P_1P_6\sin^2\left(2\sqrt{7}\tilde{c}(\nu)L\right) \tag{6}$$

with $P_1 = |E_1(0)|^2$ and $P_6 = |E_6(0)|^2$ the percentage of light coupled in each supermode and ν the light frequency. The Taylor expansion of the transmission in Eq. (6) can be expressed as

$$T(\nu) = 1 - 4P_1P_6\sin^2\left(\phi_0 + 2\pi\tau_0\nu\right). \tag{7}$$

with the phase term ϕ_0 and the delay τ_0 expressed as

$$\phi_0 = 2\sqrt{7}\tilde{c}(\nu_0)L - 2\sqrt{7}c_1L\nu_0 \tag{8}$$

#210303 - $15.00 USD Received 25 Sep 2014; revised 16 Nov 2014; accepted 21 Nov 2014; published 26 Nov 2014

$$\tau_0 = \frac{\sqrt{7}}{\pi} c_1 L \tag{9}$$

The variables ν_0 and c_1 correspond to the center frequency and the differential group delay (DGD) between modes 1 and 6.

Acknowledgments

This work is supported by ARO through grants W911NF-10-1-0441 and W911NF-12-1-0450.

#210303 - $15.00 USD Received 25 Sep 2014; revised 16 Nov 2014; accepted 21 Nov 2014; published 26 Nov 2014